Preparation and Characterization of Ni-based Catalysts Supported on Metal Organic Frameworks (MOFs) for CO_2 Conversion to Value-added Chemicals

J. Sani [1] [2]*
M.L. Mohammed [1]
A.M. Sokoto [3]
A.S. Sambo [4]

Received: 14/11/2024
Revised: 16/11/2024
Accepted: 7/12/2024

[1] Department of Energy and Applied Chemistry, Usmanu Danfodiyo University Sokoto.
[2] Sokoto Energy Research Center, Usmanu Danfodiyo University Sokoto.
[3] Department of Pure and Environmental Chemistry, Usmanu Danfodiyo University Sokoto.
[4] Department of Mechanical Engineering, Usmanu Danfodiyo University Sokoto.
* Corresponding Author's Email: jamilu.sani@udusok.edu.ng

Preparation and Characterization of Ni-based Catalysts Supported on Metal Organic Frameworks (MOFs) for CO_2 Conversion to Value-added Chemicals

J. Sani
Usmanu Danfodiyo University
Sokoto, Nigeria
jamilu.sani@udusok.edu.ng

M.L Mohammed
Usmanu Danfodiyo University
Sokoto, Nigeria

A.M Sokoto
Usmanu Danfodiyo University
Sokoto, Nigeria

A.S Sambo
Usmanu Danfodiyo University
Sokoto, Nigeria

Abstract— This research is aimed at producing Metal Organic Frameworks (MOFs) for the conversion of CO_2 to value-added chemicals using two organic linkers namely; Terephthalic acid and Triazole. Two different MOFs materials were produced via solvent-free and solvothermal synthesis. The MOFs materials were impregnated with Ni^{2+} to produce their respective Ni-based catalysts. Fourie-Transform Infrared (FTIR) characterization of MOFs and Ni-catalyst prepared via solvothermal synthesis shows absorption bands in the range of $628cm^{-1}$–$689cm^{-1}$ corresponding to O-Ni-O and Ni-N vibration, indicating the formation of coordinate bond between –COOH, -NH groups and Ni^{2+}. X-Ray diffractograms (XRD) of the prepared MOFs revealed crystalinity with different average crystallite sizes; MOF-terephthalic acid (137.9nm), catalyst-terephthalic acid (149.9nm), MOF-triazole (155.3nm) and catalyst-triazole (2.200nm) at 2θ values of 8.616550, 8.988520, 10.51650, and 33.24290 respectively. The morphologies and particle sizes of the materials were evaluated by scanning electron microscope (SEM) which reveals the flake-like shape (MOF-terephthalic acid), cuboid shape (catalyst-terephthalic acid) and rhombohedral shape for mof-triazole and catalyst-triazole respectively. The terephthalic-based materials are found to exhibit less particle sizes (213.651-228.242nm) relative to triazole-based materials (242.591-683.093nm). It was observed that the crystalinity, crystallite size and particle size of the materials increases with the impregnation of Ni^{2+} into the frameworks. In conclusion, the solvothermal synthesis approach adopted in this study proved to be more efficient than the solvent-free synthesis in producing materials with excellent properties for the conversion of CO_2 to value-added chemicals.

Keywords — : MOFs, Triazole, Catalyst, CO_2, Terephthalic acid

I. Introduction

Anthropogenic activities have resulted in the accumulation of high concentration of carbon dioxide into the atmosphere amounting to 405ppm in 2017 and projected to rise to ~570ppm by the end of the century if appropriate measures are not taken [1]. Carbondioxide being one of the major gas responsible for climate change is believed to contributes more than 70% to the global mix of greenhouse gases [2]. Consequently, global warming, a direct result of the increased concentration of carbon dioxide, is negatively affecting the global ecosystem, leading to consequences such as drought, flooding, and rising sea levels [3].

To address the aforementioned challenges, scientists and engineers accross the globe focuses on three main strategic solutions that includes; reducing the amount of CO_2 produced, storage of CO_2, and utilization of CO_2. Out of these three strategies, utilization of CO_2 is more promising due to its cheap and attractive carbon source, and its ability to produce wide range of raw materials that can be further processed to value added chemicals and fuels [1]. The utilization of CO_2 could either be by direct usage such as in microalgae production or conversion to value-added chemicals that includes methane, methanol, urea and formic acid [4].

Various utilization approaches for CO_2 such as electrochemical, thermal, photocatalytic, biochemical and chemo-enzymatic have been investigated [5][6][7][8]. However, processes such as economic feasibility, catalysts life span, low product selectivity, less yield and need for specialized reactor are reported to be a major setbacks to these approaches [2].

Recently, hydrogenation of CO_2 is proved to be more effective in addressing some of those challenges mentioned especially when hydrogen was obtained via eco-friendly source such as electrolytic splitting of water molecules instead of methane reforming process. For instance, methanol selectivity was enhanced to about 71.8% by CO_2 hydrogenation using solid solution, and zeolite membrane as catalysts [9][10]. Similarly, an excellent CO_2 conversion rate of about 85% was exhibited by Ru/MgAl catalyst [11]. Nonetheless, these catalysts are expensive, energy intensive, and have recyclability issue.

The use of metal-organic frameworks (MOFs) in converting atmospheric carbon dioxide to useful chemicals and fuels is

gaining more attention in scientific domain [12][13]. This is due to their reproducible and facile synthesis, high porosity, chemical modification, high surface area and amenability [14]. MOFs are usually produced by linking inorganic nodes which are metal ion or metallic clustes and organic linkers that are mostly carboxylates or heterocycles through coordination bonds [15]. The chemical stability of MOFs is determined by the inorganic node. Consequently, wide range of monovalent (Ag^{+}, Cu^{+}), divalent (Fe^{2+}, Cd^{2+}, Ni^{2+}), trivalent (Ga^{3+}, Sc^{3+}), and tetravalent (Zr^{4+}, Ce^{4+}) metals have been extensively studied [16][17][18][19]. Despite their several advantages over other groups, applications of divalent metal-based MOFs are hindered by their instability under hash conditions. [15]. However, this can be leverage by impregnating the metal into the frameworks structure [20]. For instance, Rungtaweevoranit [21] combined Cu nanoparticles with UiO66 for CO_2 Hydrogenation to get the dual advantage of the MOF protecting the chemically sensitive Cu nanoparticles, and a synergistically enhanced activity with 100% selectivity for methanol over CO.

Ni-based catalysts being divalent metal catalysts are advantageous in the hydrogenation process due to their high activity, low cost, and abundance in the earth's crust. Additionally, they have been known for their ability to produce smaller nanoparticles with many active sites for the reaction which makes them favourable for CO_2 methanation. Furthermore, Ni-based catalysts have been found to be effective for CO_2 methanation due to their ability to accelerate the reaction and overcome the kinetic barrier [20]. This research seminar aimed at assesment of Ni-based catalysts supported on metal organic frameworks as potential catalyst for CO_2 conversion to value-added chemicals.

II. MATERIALS AND METHODS

A. Materials

The materials and chemicals used in this research includes; Autoclave, weighing balance, centrifuge, oven, magnetic stirrer, heating mantle, furnace, 1,4-benzenedicarboxylic acid (H_2BDC), triazole, Deionized water, N-hexane, N,N-dimethylformamide (DMF), nickel nitrate hexahydrate ($Ni(NO_3)_2.6H_2O$), and Nitrogen gas (N_2).

B. Methods

1. Solvent-free syntheses of Terephthalic acid and triazole based supports

The MOFs materials were synthesized without the addition of solvent by mechanically grinding a mixture of terephthalic acid (1.3g) and nickel nitrate hexahydrate ($Ni(NO_3)_2.6H_2O$) (1.8g) (1:0.78) in a pestle and mortar for 30min. The product was then allowed to dry overnight in an oven at 150^0C. This same procedure was repeated with triazole (0.86g) (1:0.5) as organic linker.

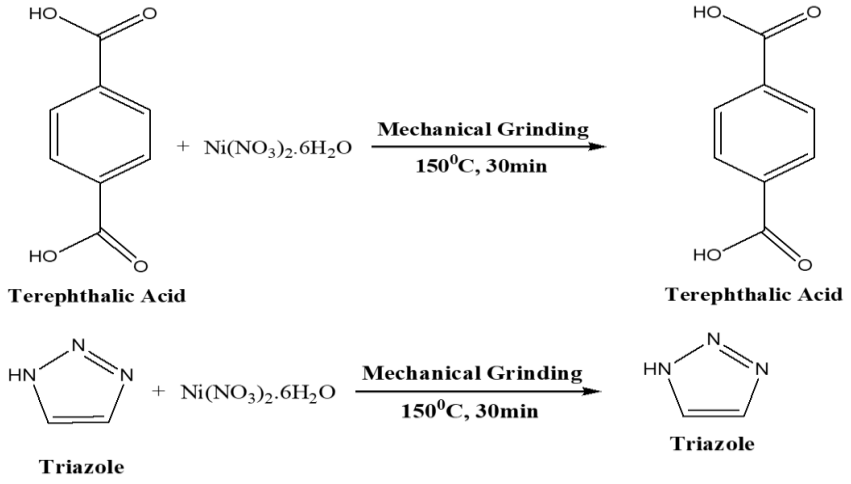

Scheme 1: Solvent-free synthesis of Metal Organic Frameworks

2. Solvothermal Syntheses of Terephthalic acid and triazole based supports

The terephthalic acid-based MOF was synthesized via the solvothermal method, following the procedure reported by Hu [22]. In this method, terephthalic acid (1,4-benzenedicarboxylic acid) (1.3g) and nickel nitrate hexahydrate ($Ni(NO_3)_2.6H_2O$) (1.8g) (1:0.78) were added to deionized water (30 cm^3) and the mixture was stirred for 5

minutes. The solution was then transferred into a 50 cm^3 autoclave and placed in an oven at 150°C for 3 days. The mixture was allowed to cool and the product washed with distilled water and dimethylformamide (DMF) which was then activated in a boiling DMF as solvent for 5h at 165^0C and dried overnight in an oven at 50^0C. The final product was then calcined at 200°C for 6 hours to remove any residual solvents. This same procedure was repeated with triazole (0.215g) as organic linker

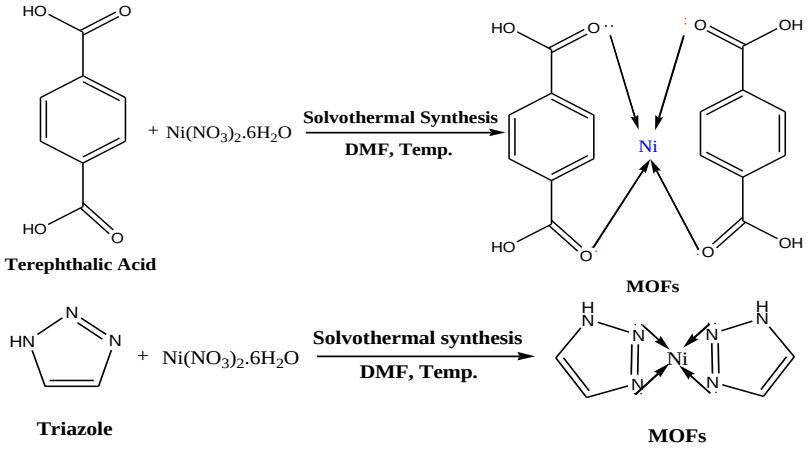

Scheme 2: Solvothermal synthesis of terephthalic acid based Mof

C. Preparation of Nickel solution (0.5M)

The nickel solution was prepared by dissolving nickel nitrate hexahydrate (3.64g) in distilled water ($25cm^3$).

D. Synthesis of Ni- supported catalysts

Encapsulation of Ni(II) precursors on the MOFs materials was carried out in accordance with the procedure reported by Zhen [23]. The calcined MOF sample (800mg) was suspended in dry n-hexane ($100cm^3$) and stirred for 30min using magnetic stirrer. Aqueos solution of Ni(II) ($6.4cm^3$) was added dropwise to the mixture with constant stirring. The resulting solution was continuosly stirred for 3h after which the solid sample was decanted, filtered and dried at room temperature. The sample was then further dried at 150^0C for 12h and calcined under inert condition of N_2 at 250^0C for 5h. This same procedure was repeated for all the synthesized MOF samples.

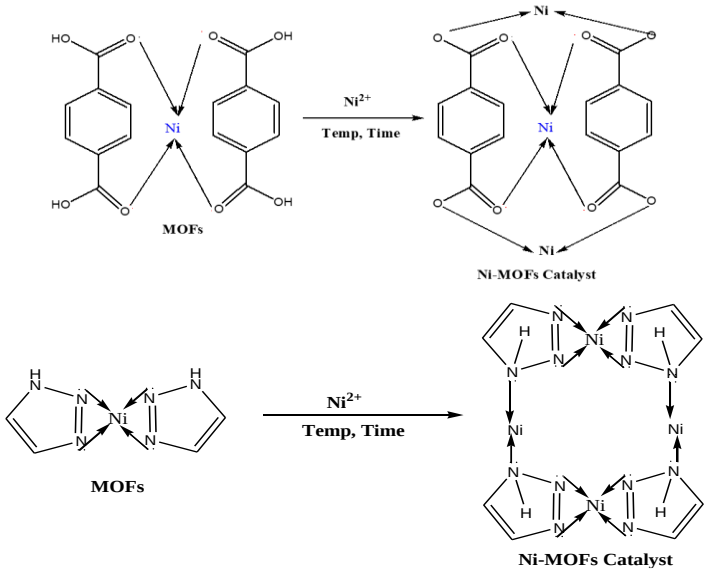

Scheme 3: Synthesis of Ni-MOF supported catalyst

E. CHARACTERIZATION OF THE SUPPORTS AND CATALYSTS

1. Fourier Transform Infrared Spectroscopy (FTIR)

The FTIR analysis was conducted using Agilent Cary 630 spectrometer in conjunction with a 5 bounce diamond ATR sampling accessories of internal reflection element (IRE) crystal. The analysis was in the transmittance mode and the signal was collected within the range 650-4000 cm^{-1} wavenumber.

2. X-ray Diffraction (XRD)

The powder x-ray diffraction (PXRD) analysis was performed using a Rigaku Miniflex 6G equipped with the Rigaku smartlab software operating at 40kV and 15mA with a Cu Kα as X-ray source. The powder samples were loaded onto a sample holder and scanned in the 2θ range of 3^0 to 90^0 at a scan rate of 10^0/min.

Crystallite size was computed using scherrer equation as shown in equation 1.

$$D = K\Lambda/\beta COS\theta \quad (1)$$

Where;

D = Average crystallite size

K = Scherrer constant

Λ = Wavelenght of radiation

B = Full width half maxima

θ = Peak position

3. Scanning Electron Microscopy (SEM)

The SEM analysis was carried out using a thermofisher scientific phenom prox desktop SEM equipped with phenom prosuite software. The sample was mounted on a sample holder and coated with a thin layer of gold using a sputter coater at a resolution of 6nm SED and 8nm BSD. Surface morphology of the sample was observed by capturing various magnifications of the images.

III. RESULTS AND DISCUSSION

Figure 1 shows absorption spectra of four different materials used in this work. Figure 1a is the spectra of Pure Terephthalic acid as obtained from the recorgnized chemical vendor, Figure 1b is the spectra of MOF synthesized from terephthalic acid without the use of any solvent. Figure 1c spectra is for the MOF synthesized from terephthalic acid via solvothermal method whereas Figure 1d is the spectra of Ni-catalyst supported on the prepared MOFs (Figure 1c)

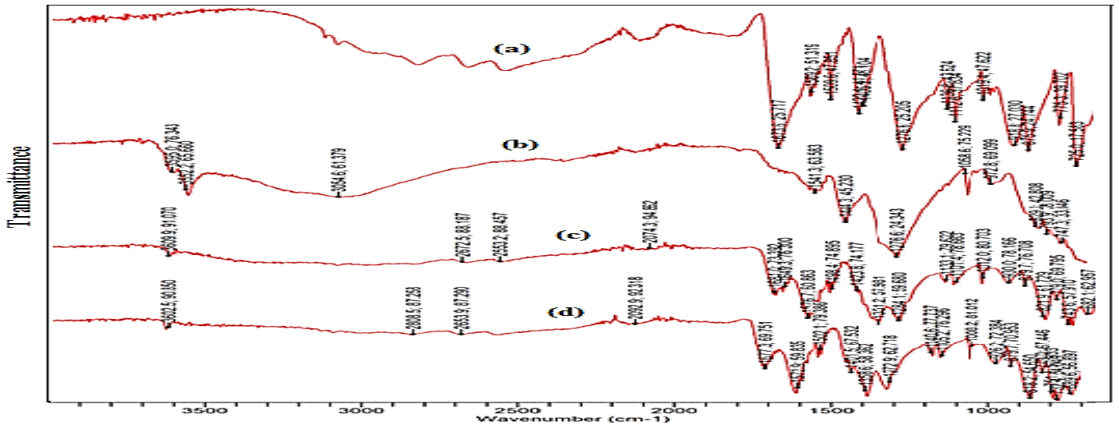

Figure 1: FTIR Spectra of (a) Pure terephthalic acid (b) Solvent-free synthesized MOF-terephthalic acid (c) Solvothermal synthesized MOF-terephthalic acid (d) Catalyst terephthalic acid

Figure 1a, shows a more intense sharp absorption peaks confirming the purity of the terephthalic acid used as ligand. The absorption observed at 1673cm^{-1} could be ascribed to C-C stretching vibration from the aromatic structure

Whereas the peaks at 918 cm^{-1}, 1424 cm^{-1}, 1276 cm^{-1}, and 725 cm^{-1} corresponds to O-H bending vibrations of the carboxylic (OOH) group, C-H bending, C-O stretching and C-H rocking respectively [24][25]. Solvent-free synthesis was employed to test its efficacy in the synthesis of MOFs-catalysts that could be used in the production of sustainable products from carbondioxide. For the solvent-free synthesis of MOFs-terephthalic acid, four major absorption peaks that were due to the O-H stretching of interlayer water (3595-3352 cm^{-1}), symmetric and assymetric stretching of carboxylate group

(1541 and 1444 cm^{-1}) were observed as shown in Figure 1b. However, in all the solvent-free syntheses (Figures 1b and 2b), no any peak relating to Ni absorption was observed. This is an indication that solvothermal synthesis is the most suitable method to be employed for the synthesis of the desired products. However, in all the MOFs-terephthalic acid and catalysts-terephthalic acid synthesized via solvothermal, absoption peaks (682 cm^{-1} and 689cm^{-1}) corresponding to O-Ni-O vibration, indicating the formation of the coordination bonding among the –COOH groups and Ni^{2+} were observed as shown in Figures 1c and 1d respectively [26]. Also, the appearance of the absorption peaks at 1575 and 1384cm^{1} corroborates to the asymmetric and symmetric vibrations of the coordinated carboxyl (−COO−) group, respectively. These peaks confirm that −COO– of terephthalic acid is coordinated with metal in a bidentate mode [27][28].

Figure 2 shows absorption spectra of four different materials used in this work. Figure 2a is the spectra of Pure triazole, Figure 2b is the spectra of MOF synthesized from triazole via solvent-free synthesis. Figure 2c spectra is for the MOF synthesized from triazole via solvothermal method whereas Figure 2d is the spectra of Ni-catalyst supported on the prepared MOFs (Figure 2c)

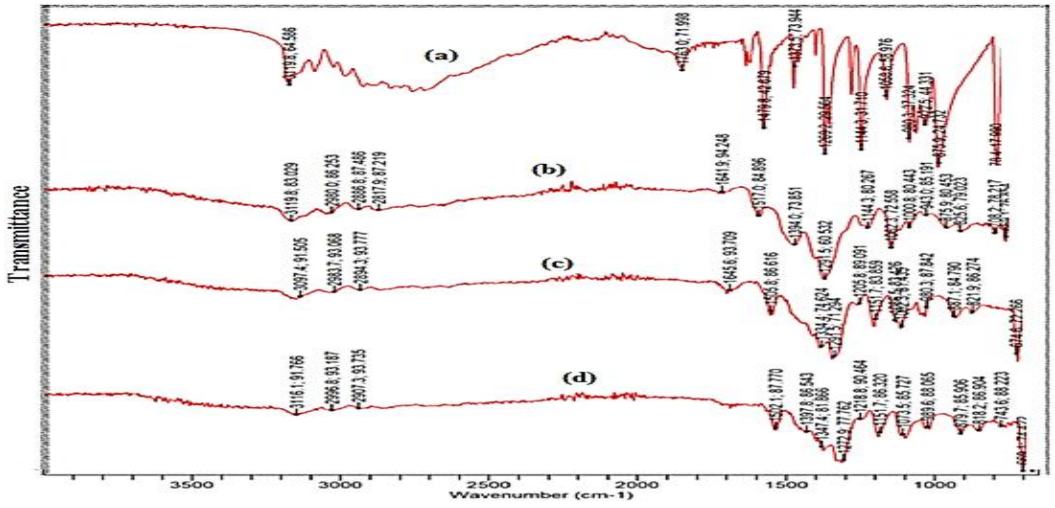

Figure 2: FTIR Spectra of (a) Pure Triazole (b) Solvent-free synthesized MOF-Triazole (c) Solvothermal synthesized MOF-Triazole (d) Catalyst Triazole

The spectra in Figure 2a shows a sharp absorptions at 3119 cm^{-1}, 1763 cm^{-1}, 1479 cm^{-1}, 1268 cm^{-1}, and 875 cm^{-1} indicating the purity of the triazole used as a ligand. The absorptions at 3119 cm^{-1} and 1763 cm^{-1} were due to N-H and -N=N stretching vibrations respectively while absorption at 1479 corresponds to C=C stretching for aromatic compounds [26]. Major absoption peaks observed in solvent-free synthesis of triazole MOFs were; 3119 cm^{-1}, 2980-2817 cm^{-1}, 1394 cm^{-1}, and 1062 cm^{-1} as shown in Figure 2b. These peaks corresponds to N-H stretching vibration (3119cm^{-1}), O-H stretching vibration due to crystal water from metal precursor (2980-2817 cm^{-1}) and C-H stretching vibration (1062 cm^{-1}). Similarly, in Figures 2c and 2d, noticeable absorption vibrations (674cm^{-1} and 669 cm^{-1}) that were due to N-Ni have been seen, confirming the formation of N-Ni linkage. The absorption bands at 1506 cm^{-1} and 1502 cm^{-1} in Figures 2c and 2d are due to the stretching vibrations of the para-aromatic C–H group in the heterocycles [28][29].

Figure 3 shows the X-ray diffractogram patterns of four different materials synthesized (MOF-triazole, MOF-terephthalic acid, catalyst triazole and catalyst terephthalic acid).

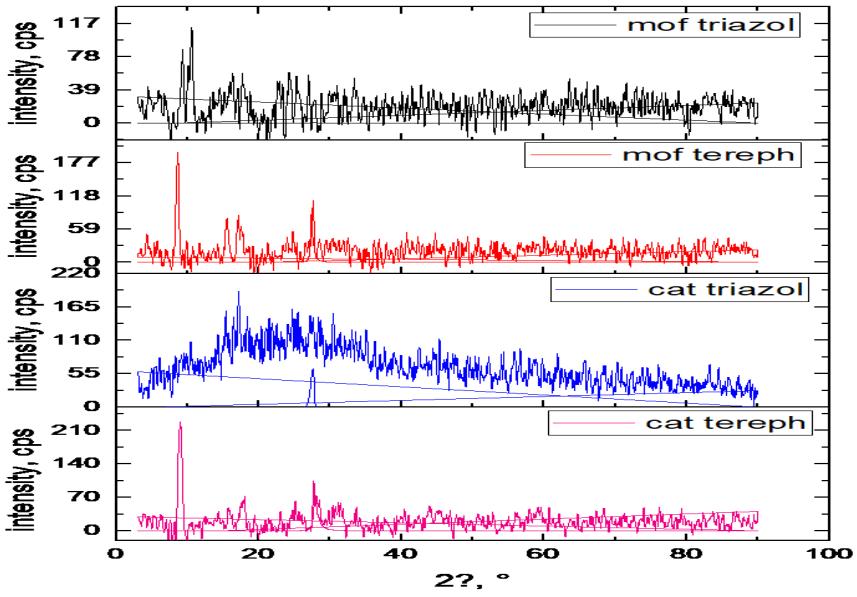

Figure 3: XRD patterns of MOF-triazole, MOF-terephthalic acid, catalyst triazole and catalyst terephthalic acid

The XRD patterns of the synthesized materials are in conformity with the well-matched diffractograms reported by Heidary [30] confirming the crystallinity of the synthesized materials. Noticeably, the main differences observed between the spectra was slightly sharp peaks in the spectra of MOF-terephthalic and MOF-triazole which were shifted to higher degree of crystallinity and large unit cell [30]. This might be attributed to the intense treatment encountered during metal-impregnation process [31]. Table 1 shows a gradual increase in the crystallite size (D) of terephthalic acid based materials. This might be due to the impregnation of metal (Ni) into the frameworks which increases the number of metal (Ni) sites [32]. However, this is in contrast to the result obtained for the triazole-based materials where a significant decrease in the crystallite size (D) was observed from MOF-triazole (155.3nm) to cat-triazole (2.20nm) respectively. This incompatibility might be due to inherent limitations in the peak profile analysis of the XRD data with the use of a width of the peak at the half of its maximum, excluding small crystallites from XRD data analysis [33].

Table 1: Crystallite size of the synthesized materials

Sample	2θ (^{0})	K	Λ	β (^{0})	D (nm)
MOF-tereph	8.61655	0.94	1.5406	0.41680	137.9
Cat tereph	8.98852	0.94	1.5406	0.55501	149.9
MOF-triazol	10.5165	0.94	1.5406	0.53654	155.3
Cat triazol	33.2429	0.94	1.5406	39.4599	2.200

Figure 4 shows the SEM images of the MOFs and catalysts used in this research.

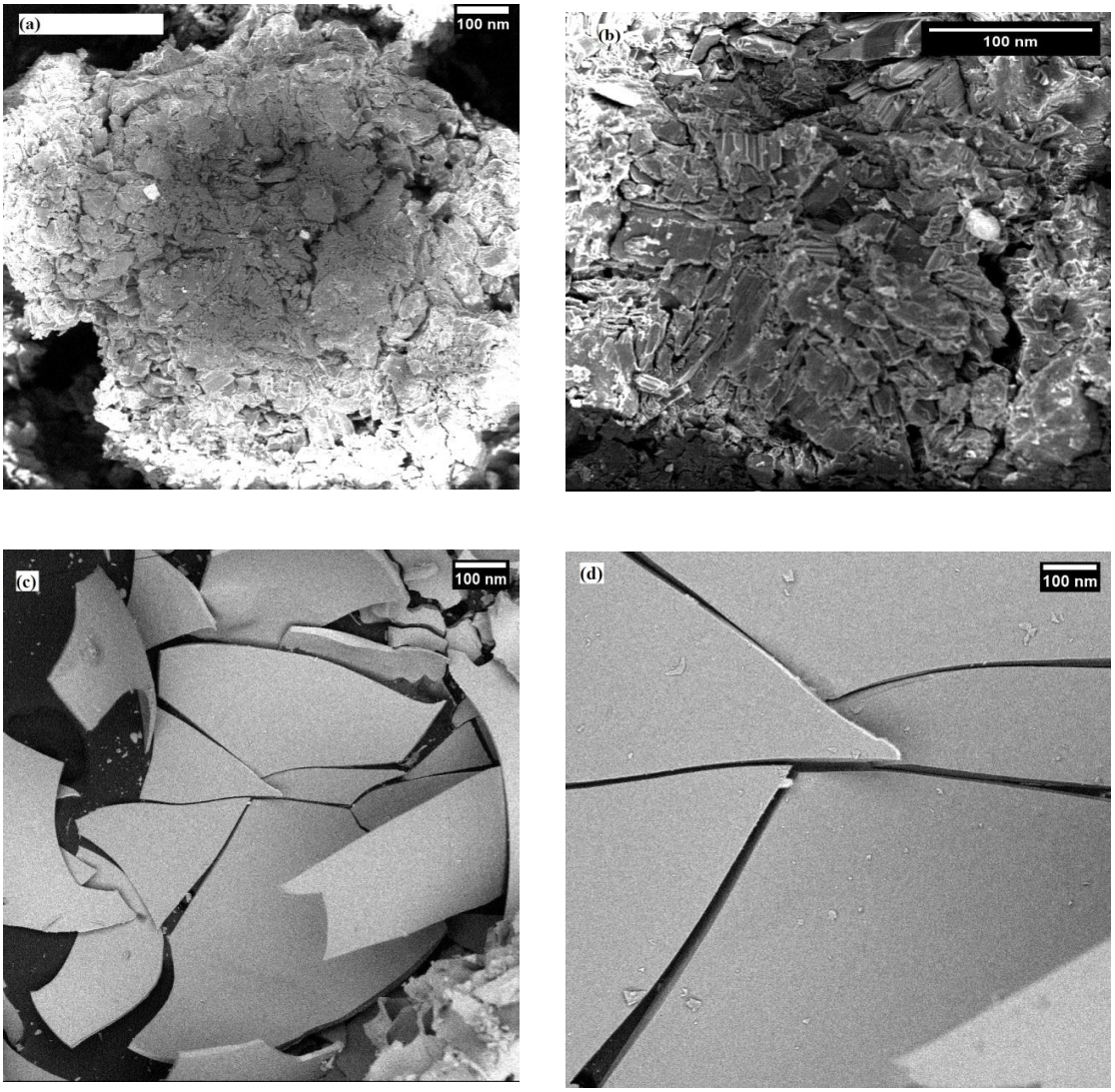

Figure 4: SEM images of (a) MOF-terephthalic acid (b) catalyst-terephthalic acid (c) MOF-triazole and (d) catalyst triazole

Scanning Electron Microscopy (SEM) was used to evaluate the morphology and average particle size as seen in Figure 4 and Table 2 respectively. The morphologies and average particle sizes of the materials were revealed depending on their different synthetic procedures. The flake-like shape was observed for MOF-terephthalic acid with less particle size (213.651nm) as compared to the cuboid shape of catalyst-terephthalic acid with high particle size (228.242nm). Similarly, the same trend in particle size (243.591nm and 683.093nm) was observed for the rhombohedral shapes of MOF-triazole and catalyst-triazole. These results corroborates with the findings of Rashed [34]. Particle size of MOF was reported to have a significant impact on its activity. For instance, study on MIL-101 MOFs investigated the effect of particle size on the catalytic activity for the conversion of CO_2 to methanol. It was observed that smaller particle sizes resulted in higher methanol production rates due to increased surface area and improved mass transfer of reactants [35]. Similarly, in the conversion of CO_2 to formic acid, it was found that reducing the particle size of HKUST-1 resulted in increased catalytic activity, attributed to the higher surface area and improved diffusion of reactants within the smaller particles [35].

Table 2: Particle size of the synthesized materials

Sample	Area(m^2)	Std Dev.	Angle(^{0})	Lenght(nm)
MOF tereph	214.375	26.455	-11.961	213.651
Cat tereph	229.036	26.436	16.454	228.242
MOF triazole	244.550	23.668	-9.588	243.591
Cat triazole	684.000	18.375	-38.636	683.093

IV. CONCLUSION

In this research, solvent-free and solvothermal syntheses routes were employed in the synthesis of different MOFs and catalysts materials using terephthalic acid and triazole as ligands. FTIR results showed that solvothermal route is the most suitable method in the synthesis of MOFs material. Furthermore, FTIR characterization confirms the formation of Ni-based MOFs and catalysts. Conclusively, flake-like, cuboid, and rhombohedral shaped materials were successfully synthesized with appreciable crystallites and particle sizes for CO_2 conversion to value-added chemicals.

ETHICAL AND COMPETING INTEREST

The authors declare that they have no known ethical or competing interests that could have influenced the work reported in this paper.

ACKNOWLEDGEMENTS

The authors graciously acknowledged the financial support provided by the petroleum Technology Development Fund (PTDF). We are equally grateful for technical support from the Centre for Advanced Science Research and Analytical Services (CASRAS), UDUS and Sokoto Energy Research Centre (SERC), UDUS.

V. REFERENCES

[1] Liu M, Yi Y, Wang L, Guo H, Bogaerts A. Hydrogenation of carbon dioxide to value-added chemicals by heterogeneous catalysis and plasma catalysis. *Catalysts*. 2019 Mar;9(3):275. doi:10.3390/catal9030275.

[2] Saravanan A, et al. A comprehensive review on different approaches for CO2 utilization and conversion pathways. *Chem Eng Sci*. 2021 Feb;236:116515. doi:10.1016/j.ces.2021.116515.

[3] Trickett CA, Helal A, Al-Maythalony AB, Yamani ZH, Cordova KE, Yaghi OM. The chemistry of metal–organic frameworks for CO2 capture, regeneration and conversion. *Nat Rev Mater*. 2017 Jul;2(8). doi:10.1038/natrevmats.2017.45.

[4] Huang CH, Tan CS. A review: CO2 utilization. *Aerosol Air Qual Res*. 2014 Jan;14(2):480–99. doi:10.4209/aaqr.2013.10.0326.

[5] Overa S, Ko BH, Zhao Y, Jiao F. Electrochemical approaches for CO2 conversion to chemicals: A journey toward practical applications. *Acc Chem Res*. 2022 Jan;55(5):638–48. doi:10.1021/acs.accounts.1c00674.

[6] Galadima A, Muraza O. Catalytic thermal conversion of CO2 into fuels: Perspective and challenges. *Renew Sustain Energy Rev*. 2019 Sep;115:109333. doi:10.1016/j.rser.2019.109333.

[7] Bhattacharya A, Selvaraj A. Photocatalytic conversion of CO2 into beneficial fuels and chemicals – A new horizon in atmospheric CO2 mitigation. *Process Saf Environ Prot*. 2021 Oct;156:256–87. doi:10.1016/j.psep.2021.10.003.

[8] Yaashikaa PR, Kumar RS, Varjani SJ, Saravanan A. A review on photochemical, biochemical and electrochemical transformation of CO2 into value-added products. *J CO2 Util*. 2019 May;33:131–47. doi:10.1016/j.jcou.2019.05.017.

[9] Wang W, Qu Z, Song L, Fu Q. Probing into the multifunctional role of copper species and reaction pathway on copper-cerium-zirconium catalysts for CO2 hydrogenation to methanol using high pressure in situ DRIFTS. *J Catal*. 2019 Dec;382:129–40. doi:10.1016/j.jcat.2019.12.022.

[10] Raso R, et al. Zeolite membranes: Comparison in the separation of H2O/H2/CO2 mixtures and test of a reactor for CO2 hydrogenation to methanol. *Catal Today*. 2020 Mar;364:270–5. doi:10.1016/j.cattod.2020.03.014.

[11] Tommasi M, Degerli SN, Ramis I, Rossetti I. Advancements in CO2 methanation: A comprehensive review of catalysis, reactor design and process optimization. *Process Saf Environ Prot*. 2023 Dec;201:457–82. doi:10.1016/j.cherd.2023.11.060.

[12] Ye J, Johnson JK. Catalytic hydrogenation of CO2 to methanol in a Lewis pair functionalized MOF. *Catal Sci Technol*. 2016 Jan;6(24):8392–405. doi:10.1039/c6cy01245k.

[13] Al-Saydeh SA, Zaidi SJ. Carbon dioxide conversion to methanol: Opportunities and fundamental challenges. *InTech eBooks*. 2018. doi:10.5772/intechopen.74779.

[14] Olajire AA. Synthesis chemistry of metal-organic frameworks for CO2 capture and conversion for sustainable energy future. *Renew Sustain Energy Rev*. 2018 May;92:570–607. doi:10.1016/j.rser.2018.04.073.

[15] Yuan S, Qin JS, Lollar CT, Zhou HC. Stable metal–organic frameworks with Group 4 metals: Current status and

trends. *ACS Cent Sci*. 2018 Mar;4(4):440–50. doi:10.1021/acscentsci.8b00073.

[16] Zhang, S. Ou, R. Ma, H. Lu, J. Holl, M.M.B. and Wang, H. "Thermally regenerable metal-organic framework with high monovalent metal ion selectivity," *Chemical Engineering Journal*, vol. 405, p. 127037, Sep. 2020, doi: 10.1016/j.cej.2020.127037. Available: https://doi.org/10.1016/j.cej.2020.127037

[17] Annamalai, J. *et al.*, "Synthesis of various dimensional metal organic frameworks (MOFs) and their hybrid composites for emerging applications – A review," *Chemosphere*, vol. 298, p. 134184, Mar. 2022, doi: 10.1016/j.chemosphere.2022.134184. Available: https://doi.org/10.1016/j.chemosphere.2022.134184

[18] Yin, C. *et al.*, "Structure-tunable trivalent Fe-Al-based bimetallic organic frameworks for arsenic removal from contaminated water," *Journal of Molecular Liquids*, vol. 346, p. 117101, Jul. 2021, doi: 10.1016/j.molliq.2021.117101. Available: https://doi.org/10.1016/j.molliq.2021.117101

[19] Li, L. *et al.*, "Synthesis and structure of metal-TCPE (metal = Th, Ce) metal-organic frameworks based on 1,2,4,5-tetrakis(4-carboxyphenyl) ethylene," *Royal Society Open Science*, vol. 9, no. 8, Aug. 2022, doi: 10.1098/rsos.220525. Available: https://doi.org/10.1098/rsos.220525

[20] Feng, F. *et al.*, "Metal organic framework derived Ni/CeO2 catalyst with highly dispersed ultra-fine Ni nanoparticles: Impregnation synthesis and the application in CO2 methanation," *Ceramics International*, vol. 47, no. 9, pp. 12366–12374, Jan. 2021, doi: 10.1016/j.ceramint.2021.01.089. Available: https://doi.org/10.1016/j.ceramint.2021.01.089

[21] Rungtaweevoranit, B. *et al.*, "Copper Nanocrystals Encapsulated in Zr-based Metal–Organic Frameworks for Highly Selective CO_2 Hydrogenation to Methanol," *Nano Letters*, vol. 16, no. 12, pp. 7645–7649, Nov. 2016, doi: 10.1021/acs.nanolett.6b03637. Available: https://doi.org/10.1021/acs.nanolett.6b03637

[22] Hu, S. Liu, M. Ding, F. Song, C. Zhang, G. and Guo, X. "Hydrothermally stable MOFs for CO_2 hydrogenation over iron-based catalyst to light olefins," *Journal of CO_2 Utilization*, vol. 15, pp. 89–95, Mar. 2016, doi: 10.1016/j.jcou.2016.02.009. Available: https://doi.org/10.1016/j.jcou.2016.02.009

[23] Zhen, W. *et al.*, "Enhancing activity for carbon dioxide methanation by encapsulating (1 1 1) facet Ni particle in metal–organic frameworks at low temperature," *Journal of Catalysis*, vol. 348, pp. 200–211, Mar. 2017, doi: 10.1016/j.jcat.2017.02.031. Available: https://doi.org/10.1016/j.jcat.2017.02.031

[24] Liu, X. "6.3 IR Spectrum and Characteristic Absorption Bands," *Pressbooks*, Dec. 09, 2021. Available: https://kpu.pressbooks.pub/organicchemistry/chapter/6-3-ir-spectrum-and-characteristic-absorption-bands/

[25] Agostini, I. Ciuffi, B. Gallorini, R.. Rizzo, A.M Chiaramonti, D. and Rosi, L. "Recovery of Terephthalic Acid from Densified Post-consumer Plastic Mix by HTL Process," *Molecules*, vol. 27, no. 20, p. 7112, Oct. 2022, doi: 10.3390/molecules27207112. Available: https://doi.org/10.3390/molecules27207112

[26] Trivedi, M.K Trivedi, A.B.D and Bairwa, H.S.K. "Fourier Transform Infrared and Ultraviolet-Visible Spectroscopic Characterization of Biofield Treated Salicylic Acid and Sparfloxacin," *Natural Products Chemistry & Research*, vol. 03, no. 05, Jan. 2015, doi: 10.4172/2329-6836.1000186. Available: https://doi.org/10.4172/2329-6836.1000186

[27] Cheng, J. *et al.*, "Ni-based metal–organic frameworks prepared with terephthalic acid hydroxylation converted methyl palmitate into jet-fuel range hydrocarbons in CO_2 atmosphere," *Fuel*, vol. 318, p. 123679, Feb. 2022, doi: 10.1016/j.fuel.2022.123679. Available: https://doi.org/10.1016/j.fuel.2022.123679

[28] Zhou, X. *et al.*, "Novel Binary Ni-Based Mixed Metal–Organic Framework Nanosheets Materials and Their High Optical Power Limiting," *ACS Omega*, vol. 7, no. 12, pp. 10429–10437, Mar. 2022, doi: 10.1021/acsomega.1c07196. Available: https://doi.org/10.1021/acsomega.1c07196

[29] Wang, K. *et al.*, "Boosting the performance of broccoli-like Ni-triazole frameworks through a CNTs conductive-matrix," *RSC Advances*, vol. 9, no. 44, pp. 25697–25702, Jan. 2019, doi: 10.1039/c9ra05442a. Available: https://doi.org/10.1039/c9ra05442a

[30] Heidary, N. Chartrand, D. Guiet, A. and Kornienko, N. "Rational incorporation of defects within metal–organic frameworks generates highly active electrocatalytic sites," *Chemical Science*, vol. 12, no. 21, pp. 7324–7333, Jan. 2021, doi: 10.1039/d1sc00573a. Available: https://doi.org/10.1039/d1sc00573a

[31] Ding, M. Flaig, R.W. Jiang, H.L. and Yaghi, O.M. "Carbon capture and conversion using metal–organic frameworks and MOF-based materials," *Chemical Society Reviews*, vol. 48, no. 10, pp. 2783–2828, Jan. 2019, doi: 10.1039/c8cs00829a. Available: https://doi.org/10.1039/c8cs00829a

[32] Chary,K. V. R. Naresh, D. Vishwanathan, V. Sadakane, M. and Ueda, W. "Vapour phase hydrogenation of phenol over Pd/C catalysts: A relationship between dispersion, metal area and hydrogenation activity," *Catalysis Communications*, vol. 8, no. 3, pp. 471–477, Aug. 2006.

[33] Słowik, G. Gawryszuk-Rżysko, A. Greluk, M. and Machocki, A. "Estimation of Average Crystallites Size of Active Phase in Ceria-Supported Cobalt-Based Catalysts by Hydrogen Chemisorption vs TEM and XRD Methods," *Catalysis Letters*, vol. 146, no. 10, pp. 2173–2184, Aug. 2016, doi: 10.1007/s10562-016-1843-1. Available: https://doi.org/10.1007/s10562-016-1843-1

[34] Rashed,A. E. Nasser, A. Elkady, M.F.Matsushita, Y. and El-Moneim, A.A. "Fe Nanoparticle Size Control of the Fe-MOF-Derived Catalyst Using a Solvothermal Method: Effect on FTS Activity and Olefin Production," *ACS Omega*, vol. 7, no. 10, pp. 8403–8419, Feb. 2022, doi: 10.1021/acsomega.1c05927. Available: https://doi.org/10.1021/acsomega.1c05927

[35] Dhakshinamoorthy, A. Asiri, A.M. and Garcia, H. "Tuneable nature of metal organic frameworks as heterogeneous solid catalysts for alcohol oxidation," *Chemical Communications*, vol. 53, no. 79, pp. 10851–10869, Jan. 2017, doi: 10.1039/c7cc05927b. Available: https://doi.org/10.1039/c7cc05927b